



Original article

**Recycling Tungsten Heavy Alloy Scrap via Ultrasonic Waves to form new ones by Powder Metallurgy Route**

H. M. Zidan<sup>1\*</sup>, Nora M. Hilal<sup>2</sup>, Mona F. Amin<sup>2</sup>, G. M. A. Elhefnawy<sup>3</sup>, Ahmed O. Abdel-Mawla<sup>1</sup>, Omayma A. El-Kady<sup>1</sup>

<sup>1</sup>Powder Technology Division, Central Metallurgical R&D Institute (CMRDI), Egypt.

<sup>2</sup>Department of Chemistry, Faculty of Science, Al Azhar University (Girls), Cairo, Egypt.

<sup>3</sup>Ultrasonic Metrology Department, National Institute of Standards, Giza, Egypt.

ARTICLE INFO

Received 06/07/2024  
Revised 19/08/2024  
Accepted --/--/2024

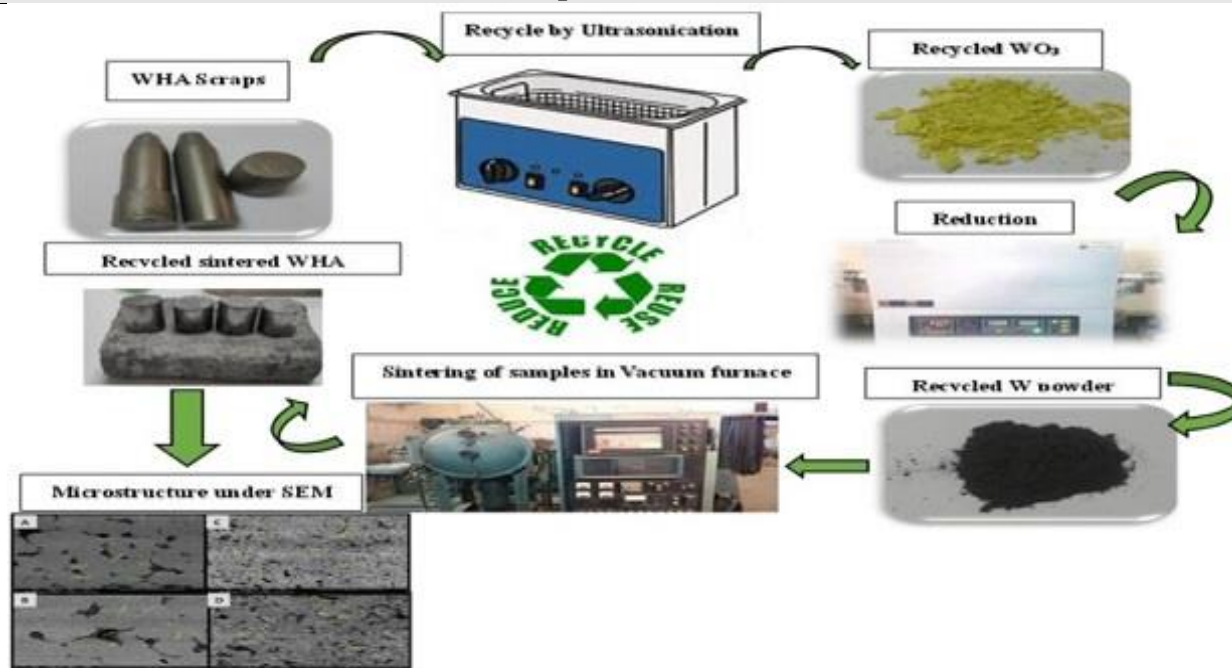
Keywords

Recycling  
Sonochemistry  
Tungsten heavy alloy  
Powder metallurgy  
Ultrasonic Non-destructive test

ABSTRACT

Ultrasonic waves with a frequency of 25 KHz were used to enhance the acidic chemical recycling of tungsten heavy alloy (WHA) scrap class 2 HA175 with a typical composition of Ni-5.25 wt%, Fe-2.25 wt%, and W-92.5 wt% to recover the tungsten powder. The experiment demonstrated that the scrap sample exposed to ultrasonic waves produced a significantly higher amount of tungsten powder with a submicron particle size. The recycled tungsten powder was utilized to manufacture a new tungsten heavy alloy sample class 2 HA175 with the same alloy composition as the above. The elemental powders were mixed mechanically, cold compacted, and sintered at 1500°C in a vacuum furnace. The microstructure, phase structure, and composition of the sintered WHAs were investigated by Scanning Electron Microscopy (SEM) and X-ray diffractometer (XRD). The recycled sample's density and hardness were higher than the original, in which the hardness increased from 312 to 340 HV, whereas the wear rate and coefficient of friction were decreased by about 50%. The longitudinal (VL) and shear (VS) velocities for both samples were examined using ultrasonic (NDT).

Graphical abstract



\* Corresponding author

E-mail address: [hadiermohammed32@outlook.com](mailto:hadiermohammed32@outlook.com)

DOI: [10.21608/IJTAR.2024.298408.1077](https://doi.org/10.21608/IJTAR.2024.298408.1077)

## 1. Introduction

Tungsten heavy alloys have attractive physical and mechanical qualities; thus, they are frequently utilized in the military (e.g., kinetic energy penetrators), nuclear radiation protection shields (e.g., vial shield, isotope container), resistance welding electrodes, and weight balancing [1]. Heavy alloys based on tungsten are two-phase metal matrix composites that usually include a composition of nickel, iron, copper, and/or cobalt mixed in with 90% to 98% tungsten [2]. Three types of scrap are produced during the production of these alloys: powder, turnings, and faulty solid. Recycling from these wastes is crucial to meeting the demand for this strategic metal since tungsten, which is expensive, makes up the majority of the scrap. Several methods are available for recovering tungsten metal from tungsten base waste alloys, including electro-leaching, soda roasting and leaching, acidic leaching, fine gravity separation, and high-intensity magnetic separation techniques [3]. OG Kuznetsova used the electrochemical process to accelerate the dissolution rate to heavy tungsten alloy wastes (wt% W 78.8, Ni 15.2, Fe 6) and get a micro dispersed electrolytic sludge powder based on nickel and iron oxides containing up to 2wt% tungsten [4].

L. Luo successfully extracted tungsten and vanadium from a sodium tungstate solution with a concentration of 95 g/l  $WO_3$ , 0.175 g/l V, and some impurities. The solution was derived from roasting tungsten alloy scrap and then dissolving it in an alkali solution. The extraction process was divided into three stages: separating and purifying vanadium from tungsten, recovering vanadium, and recovering tungsten. For tungsten recovery, the sodium salt was transformed into calcium salt following the purification of the sodium tungsten solution. Then, the  $CaWO_4$  was converted to  $H_2WO_4$  using hydrochloric acid, followed by dissolving in ammonium hydroxide and crystallizing APT, the yield of tungsten recovered was greater than 85%. [5]. Magnetic separation is a common method used in the beneficiation process of wolframite. To achieve optimal recovery of wolframite, it is typically carried out in a high-intensity magnetic separation system. Like gravity separation, particle size plays a crucial role in the conventional magnetic separation process. When the particle size of wolframite is decreased, the magnetic force acting on the particle diminishes rapidly and cannot withstand hydrodynamic drag, resulting in the loss of the fine fraction of wolframite to the tailings [6]. S.S. Kalyan Kamal used acidic leaching to recover tungsten nanocrystal powder from heavy alloy scrap with a nominal composition (Ni-7wt%, Fe-3wt%, and W-90%) [7].

In this research, a new method is used to recycle the scrapes of heavy tungsten alloy to obtain the largest yield of ultra-fine tungsten powder. This was done by stimulating and accelerating the chemical reaction on the waste using ultrasound called the sonochemistry method. Ultrasound with a frequency ranging from 20 to 100 kilohertz is frequently used in chemistry to induce chemical changes without directly interacting with molecules. Instead, the energy produced by ultrasound causes cavitation, leading to extreme temperatures and pressures in the liquid where the reaction occurs. Additionally, ultrasound can break up solids and remove

passivating layers of inert material, thereby providing a larger surface area for the reaction to occur. As a result, the reaction becomes faster due to these effects [8, 9].

The tungsten-heavy alloys correspond to class 2 grade HA175 according to ASTM B777-15. with a defined Ni/Fe ratio have been investigated in this study. The recycling of WHAs was done previously by a traditional chemical technique which consumes a large time and chemicals and produces a small yield. So, in this work, using the ultrasonic waves for the first time reduces the time and the economic cost and gives a high tungsten yield. Consequently, this paper aims to study the effect of ultrasonic waves in the recycling process of HA175 tungsten heavy alloy scraps and to use the recycled submicron tungsten powder in the fabrication of WHA with the same grade of the scrap HA175 and compare the microstructure, physical and mechanical properties of both samples; the original sample (came from the scrap) and the recycled one.

## 2. Experimental Work:

### 2.1. Recycling of the tungsten powder from WHAs scrap by a chemical process with and without ultrasonic waves

The scraps of Tungsten Heavy Alloy (HA175) shown in Fig.1 with a chemical composition of Ni-5.25 wt%, Fe-2.25 wt%, and W-92.5 wt% manufactured by powder metallurgy route in the powder technology department in CMRDI-Egypt were collected. To study the effect of ultrasonication on the yield of the tungsten powder recycled from 200 grams of tungsten heavy alloy scrapes (WHAs) were weighted and divided evenly into two groups each one (100gm) was immersed in 500ml plastic beaker (due to using of HF acid in the recycling process in the recycling process) contains acidic solution, with the following composition (50 ml Hydrochloric acid, 20 ml Nitric acid, 10 ml Hydrofluoric acid) [7].

The first group was placed in an Elma Transonic multi-frequency ultrasonic cleaning unit Mod1 (TI - H 15 MF 2) with a frequency of 25 KHz for the coarse cleaning. at the same time, the second group was exposed to the acidic medium without the ultrasonication. The reaction was left to take place in the acidic solution for one week while the samples were exposed to the ultrasound waves for only five hours per day.

After one week the dissolved scrap was diluted with 700 ml of deionized water to remove both Ni and Fe in the form of a soluble salt solution. The yellow precipitate was collected through a filtration process and washed twice with dilute HCl to remove any traces of Ni and Fe. Tungsten oxide powder was obtained through the above process and subjected to a hydrogen reduction cycle in a tube furnace.

The hydrogen-reduction cycle of  $WO_3$  showed that the complete reduction of tungsten oxide ( $WO_3$ ) to tungsten metal (W) was established at 800 °C with a holding time of 2 hours. An intermediate product  $WO_{2.72}$  (at 520 °C) and WO (at 600 °C) were formed [10]. Figure 1 shows the transformation shapes of the WHA from scrape to tungsten oxide until it reaches the Recycled Tungsten powder.

The tungsten powder resulting from the reduction process was analyzed using energy dispersive X-ray spectroscopy (SEM/EDX) microscope model TESCAN SEM VEGA3 and was investigated by x-ray diffraction analysis (XRD) using x-ray diffractometer model x, pert PRO PANalytical with cu  $\alpha$  radiation ( $\lambda = 0.15406$

nm) to determine its purity and the percentage of oxygen in it. The recycled powders from the sound waves and those without the influence of ultrasonication after reduction were investigated by scanning electron microscope to study the difference in granular size and shape between them.



## 2.2 Manufacturing of tungsten heavy alloy from recycled tungsten powder

After ensuring that the recycled tungsten powder contains a very small percentage of oxygen (less than 2%), it was used in the manufacturing of class 2 tungsten heavy alloy Grade HA175 which is the same grade as the scrap alloy. The grain size of elemental powders (Iron and Nickel) ranges from 2 up to 10  $\mu\text{m}$  with 99.8% purity. The chemical composition of the alloy is 92.5% Recycled tungsten(W), 5.25% Nickel (Ni), and 2.25% Iron (Fe). All chemicals were supplied from El-Gomhoria Company for Chemicals - Cairo- Egypt. The elementary powders of the WHA were mixed in a planetary ball mill at 300 rpm speed for 6 hours. 1.5 wt % hexane was added during the mechanical milling as a process controlling agent (PCA) to decrease the cold-welding effect during the milling process. The ball-to-powder ratio was 5:1 and the milling process occurred under argon gas to protect the metal powders from any oxidation. The mixed powders were blended with 1.5 wt% paraffin wax and cold compacted using a uni-axial Hydraulic press under compaction pressure of 70 bar with a 10mm diameter. The green compacts were sintered using a liquid phase sintering cycle at a temperature of 1500°C for 1 h in a vacuum furnace there is a 30-minute holding time at 250°C to get rid of paraffin wax from the samples.

## 3. Characterization

### 3.1 The Characterization of Reduced Recycled Powder

The particle size-distribution of recycled tungsten powder with the ultrasonic wave and without ultrasonic wave was measured by DLS (dynamic light scattering) using Zetasizer Nano ZS-90 Model ZEN3600 (Malvern Panalytical Ltd; Spectris). Also, the shape and particle size were determined by the Scanning electron microscope model TESCAN SEM VEGA3. The purity of the power was estimated by EDS (Energy-dispersive X-ray spectroscopy) and XRD (x-ray diffractometer model x, pert PRO PANalytical)

### 3.2 Density measurements

The density of the sintered specimens was measured by Archimedes water immersion method according to MPIF standards 42, 1998, The density of samples was calculated according to the following equation Eq .1.

$$\text{Density}(\text{gm}/\text{cm}^3) = \frac{\text{Wight of sample in air}}{(\text{Wight of sample in air} - \text{Wight of sample in water})} \quad (1)$$

### 3.3 Phase composition and microstructure identification

To estimate the phase structure and composition of the original and recycled samples were investigated by x-ray diffraction analysis (XRD) using x-ray diffractometer model x, pert PRO PANalytical with Cu  $\alpha$  radiation ( $\lambda = 0.15406$  nm). For microstructure investigation, the surfaces of the sintered samples were prepared by grinding and polishing using silicon carbide papers with different grits (80, 400, 600,800,100,1200, and 20000respectively) and finally with alumina paste. The etching process for the sample surfaces was done by the etchants illustrated in Table 1. to clarify the grain boundaries and particle shape [11].

The metallographic structure of the sintered specimens was examined using the scanning electron microscope (SEM) model TESCAN SEM VEGA3.

**Table 1.** Etchant parameters for the sintered samples

Phase	The etching composite	Time
Etchant for	10g Potassium Ferri-cyanide	2 Minutes
W-phase	10g NaOH	
	500ml H <sub>2</sub> O	
Etchant for	10g ammonium persulfate	4 Minutes
Y-phase	100ml H <sub>2</sub> O	

### 3.4 Mechanical properties

#### 3.4.1 Hardness test

The hardness of both samples was measured by Vickers hardness tester type LalZhou Welyl, model HV-30MPTA, using a 5 Kg load for 20 seconds. An average of three hardness readings, for each specimen, was determined.

#### 3.4.2 Tribological properties (Wear rate and the friction coefficient)

The tribological test was applied to the cylinder-polished samples (10 mm diameter and 8mm high) using a (pin-on-disk) tester machine that works according to the SAE-J661 Standard Test(12). The disk is made from alloyed steel with a hardness of 65 HRC. The friction coefficient of the samples is detected under 20 N and 30N friction force, 120 rpm speed of the disc, and 830 sliding distances. The specific wear rate was detected by using the same pin on the disk machine. It depends on the sample's weight loss with time. It was measured under 20N and 30N applied force on the sample and 10 min time for each sample.

#### 3.4.3 Ultrasonic measurements

Ultrasonic pulse-echo technique, an ultrasonic flaw detector (GE, USM36) connected with a 4 MHz longitudinal transducer (Karl Deutsch S12 HB4) and a 2 MHz shear transducer (Krautkramer K2KY) was used to measure the ultrasonic longitudinal VL and shear VS velocities [13]. To calculate the elastic moduli such as longitudinal (L), shear (G), bulk (B), Young's (Y), and Poisson's ratio the calculated ultrasonic longitudinal VL and shear VS velocities were used [14].

$$L = \rho V_l^2, \tag{2}$$

$$G = \rho V_s^2, \tag{3}$$

$$B = L - \left(\frac{4G}{3}\right), \tag{4}$$

$$\nu = \left(\frac{L-2G}{2(L-G)}\right), \tag{5}$$

$$Y = (1 + \nu)2G, \tag{6}$$

## 4. Results and discussions

### 4.1 Characterization of the recycled tungsten powder with and without ultrasonic waves

#### 4.1.1 Estimation of the yield of tungsten powder

The tungsten powder yield in grams with ultrasonic waves is 20 gm and without ultrasonic waves is 1.7 gm. This quantity results from an entire week of acids reacting with scrap. According to the results, the percentage of extracted tungsten under the effect of ultrasound waves is approximately nine times more than the percentage eliminated without the influence of ultrasound waves. The reason for that is the passivation of the tungsten in the acidic medium and the alloy stopped dissolving as a passivating film grows. [15]So, the oxidation rate of the alloy wastes slows down. Acids are prevented from penetrating the core and interacting with a different metal layer by this passive layer. However, ultrasonic waves have a significant impact on this layer because they break it down, which aids in the continuation of the oxidation process on the waste and produces more powder in a shorter length of time. Figure 2 is an economic indicator for the recycling process of WHAs which indicates that this method is more economical for the production of the tungsten metal from its scrap. Where, the actual price of one kilogram of W metal is about 700 dollars, while the current price in the international market ranges from 1850 to 9000 dollars according to the particle size & purity.

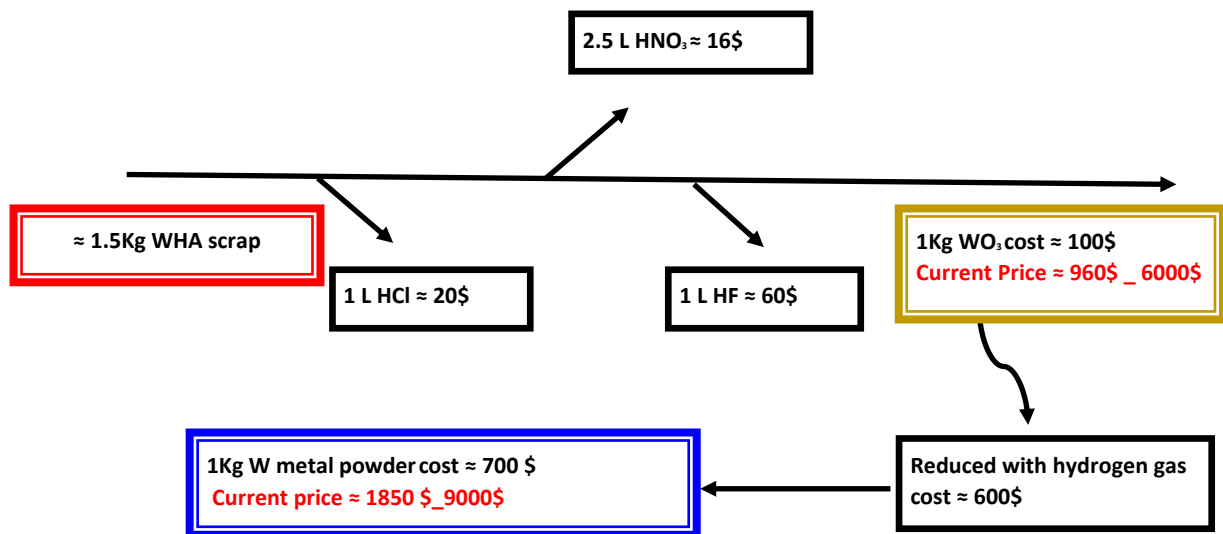


Fig 2 Schematic diagram for the economic study of the recycling process of WHAs

#### 4.1.2 Microstructure investigation of the recycled tungsten powders

##### 1) Comparison between tungsten powder particle size

Figure 3. shows the analysis of particle size distribution by DLS it indicates that the size distribution by

intensity has one peak for each tungsten-reduced powder, Figure 3 (A) recorded the peak at 1599 nm and the z-average was recorded as 4086 nm for the reduced tungsten powder that was recycled without using ultrasonic waves. Figure 3 (B) recorded a peak at 576.5 nm

and the z-average was recorded as 1590 nm for the reduced tungsten powder that was recycled with the aid of ultrasonic waves.

This indicates that the effect of ultrasound led to a significant reduction in the granular size and made it finer.

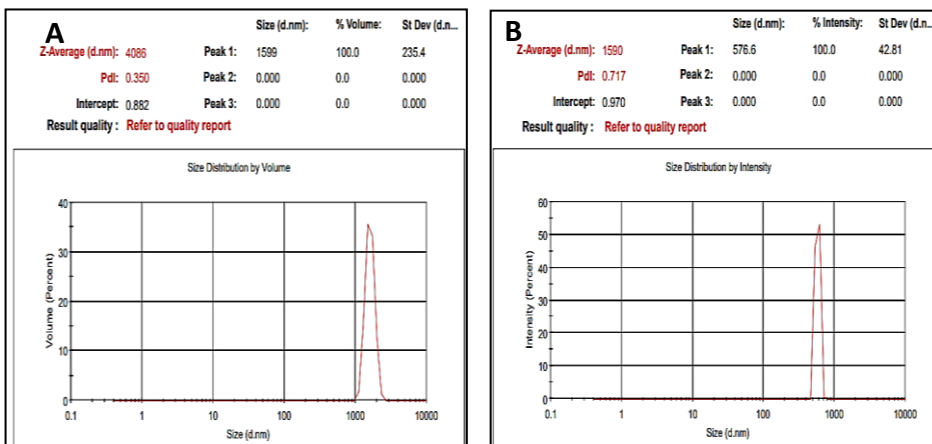


Figure 3. Measurement of particle size-distribution by DLS using Zetasizer Nano for the recycled tungsten powder after reduction, A) without ultrasonic wave, B) with ultrasonic wave

Figure 4. shows the particle shape and size of the produced recycled tungsten powder. The W powder yield from the traditional chemical method has a large particle size ranging from 1.601µm to 2.361µm as shown in Figure 4 (A) while the ultrasonicated has more fine particles with 1.304 to 0.5797 µm. This is due to the effect of high vibration of the ultrasonic waves that helps in the breakdown of the aggregates and makes more grain refinement [16]. Consequently, when this powder is used to fabricate a new WHA, this WHA sample has enhanced mechanical and physical properties.

2) The EDS analysis of the reduced tungsten powder

The EDS analysis is shown in Figure 5. reveals that the percentage of oxygen in the tungsten powder after the reduction process is less than 2%, which makes it a suitable powder for entering the process of manufacturing tungsten heavy alloys or any other alloy that contains tungsten in its metallic powder form. This may be attributed to the good reduction parameters for the tungsten oxide prepared from the ultrasonic technique.

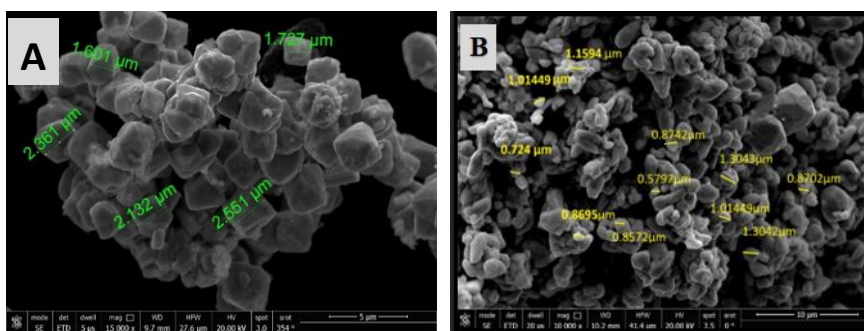


Figure 4. The recycled tungsten powder after reduction, A) recycled without the effect of ultrasonic wave, B) recycled under the effect of ultrasonic wave

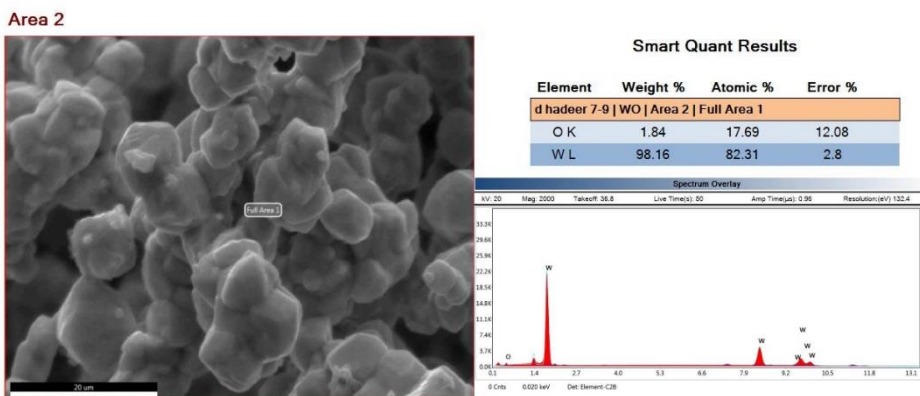


Figure 5. The EDS of the recycled tungsten powder after reduction

### 3) XRD pattern of the reduced tungsten powder

The XRD pattern of the recycled ultra-sonicated tungsten metal powder (W) is observed in the XRD patterns in Figure 6. The reflection main peaks corresponding to (W) are characterized at  $40.285^\circ$ ,  $58.278^\circ$ , and  $73.215^\circ$  were achieved which are the mean fingerprint peaks for W. This demonstrates that the recycling and reduction procedure was successful and the reduction temperature which was  $800^\circ\text{C}$  is suitable for the total conversion of  $\text{WO}_3$  to W powder is free from any contaminants or oxidation, also the sharp peaks corresponding to W refers to the high crystallinity of the prepared W powder.

#### 4.2.2 X-ray diffraction phase structure and composition

Figure 8 shows the XRD pattern of both the original and the ultrasonicated recycled samples. The primary peaks correspond to the BCC-structured tungsten phase (which is in excellent agreement with the data from JCPDS file No. 04-0806) and very weak two peaks relating to the Ni-Fe solid solution phase. This indicates that the recycled sample has the same chemical composition as the original one without any foreign phases or oxide peaks recorded for both samples. Also, this is attributed to the good mechanical milling and sintering parameters.

### 4.3 Microstructure analysis

#### 4.3.1 The microstructure investigation by scanning electron microscope (SEM)

Figure 9 shows the SEM of the sintered samples, in which A & B belong to the original WHA sample at 2000x and 4000x respectively, and C&D corresponds to the recycled WHA sample at 2000x and 4000x respectively. It is clear that the average grain size of tungsten particles, as their size in the original sample ranges from  $32\mu\text{m}$  to  $9\mu\text{m}$  while in the recycled sample it ranged between  $11\mu\text{m}$  to  $1.5\mu\text{m}$ . This indicates that the grain refinement of the recycled W particles is due to the effect of ultrasonication. Also, it can be observed that Fe and Ni are more homogeneously distributed in the W matrix of the recycled sample than in the original one. It was noticed that the original sample had more pores than the recycled sample. This is related to the good densification of the fine particles with each other during the compaction and sintering processes [18].

#### 4.4 Hardness measurement

The Hardness values of the original WHA and the recycled one are 312 and 340 HV respectively. The results show a significant increase in the hardness value of the recycled sample. That can be explained from three points of view, the first is the manufacturing of WHA sample from the finer recycled W metal, the presence of submicron powder has a good effect on the improvement of the mechanical properties, especially the hardness [19]. This is due to the good entrance of the nanoparticles in the voids and vacancies of the matrix which hinder the insertion of the hardness indenter in the sample so the hardness values increase. The second reason is the good mechanical milling parameters which leads

to a homogeneous distribution of all the sample constituents with each other's. The third is the general reduction of the particle size which enhances the total hardness of the sample according to the Hall-Petch equation which states that the hardness value is reversible with the particle size.

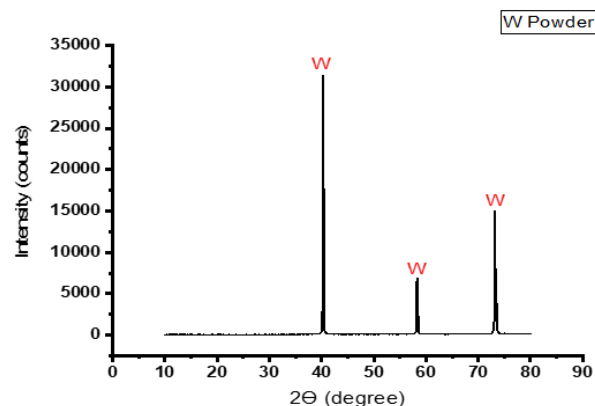


Figure 6. The XRD pattern of the recycled tungsten powder after the reduction process

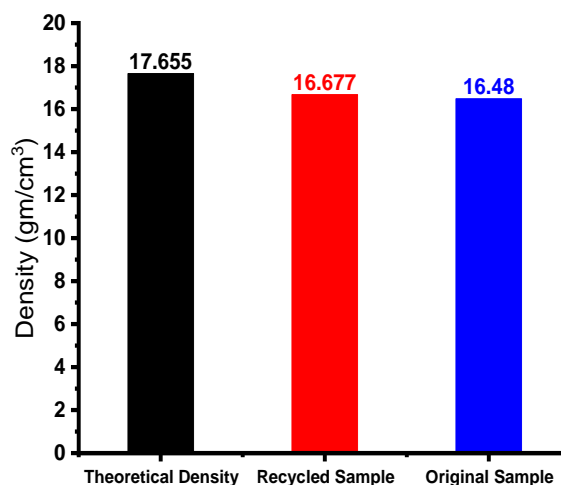


Figure 7. The density of original and recycled WHA sintered samples

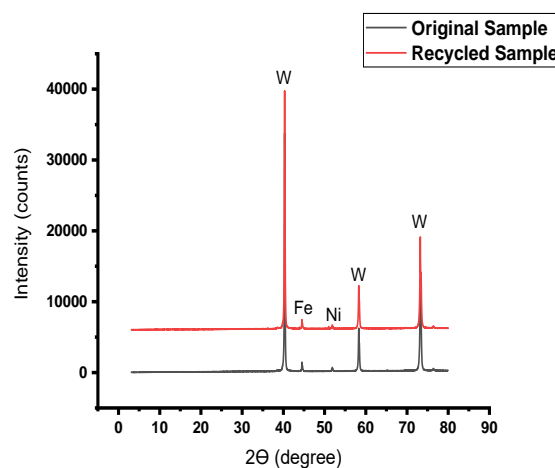


Figure 8. The XRD pattern of original and recycled sintered tungsten heavy alloy (WHA)

4.5 Wear and friction coefficient

4.5.1 Wear test

Figure 10 shows the specific wear rate of both original and recycled samples under 20 and 30 N loads. The specific wear rate (k) was calculated according to Eq. 7, where the mass change ( $\Delta m$ ) as the pin (sample) traveled divided by normal load (F), material density ( $\rho$ ), and sliding distance(S). [20]

$$k = \frac{\Delta m}{\rho \cdot S \cdot F} \quad (7)$$

The results show that there is a noticeable improvement in the specific wear resistance, as the presence of ultra-fine tungsten particles in the recycled sample assisted to improve the mechanical properties and significantly reduce the wear rate when compared with the original sample, which contains larger tungsten particles. Also, the increases in the wear resistance are due to the good interaction and diffusion of particles with each other. This follows the density and hardness results, in which the high-densified sample with a high hardness has good wear and friction resistance. Also, when the applied load increases from 20 to 30N the fracture of the particles takes place which causes more weight loss.

4.5.2 Coefficient of friction

The variation in the friction coefficient with time is shown in Table 3. The coefficient of friction of the original sample is higher than the recycled one. The reason for that is the large particle size of tungsten in this sample which can be removed from the sample surface more easily than the other one. The dislocated particles generated micro-voids, which roughened the surface and subsequently increased the friction. On the other hand, the fine grains in the recycled sample were compacted strongly with each other in a good manner that prevents them from being removable from the surface. For high loads, more friction occurs and more particles are removed from the original sample surface which is considered the pin of the wear device.

4.6 Ultrasonic waves and mechanical characterizations

Table 4. shows the propagation of ultrasound waves through the original sample with low longitudinal ( $V_l$ ) and shear ( $V_s$ ) velocities, in contrast to the results of the produced velocities from the passage of ultrasound waves in the recycled sample. The recycled sample's high density and small grain size allow the waves to pass smoothly through it.

As opposed to the original sample's large grain size and pores, which caused the waves to be scattered inside it. Therefore, the ultrasonic velocities were reduced [14].

This rise in velocities indicates an increase in the mechanical properties, which is evident in the higher

**Table 3.** VL, VS, Poisson's ratio ( $\nu$ ), longitudinal modulus (L), shear modulus (G), bulk modulus (B), and young modulus (Y) of both original and recycled samples.

Samples	$V_l$ [m/s]	$V_s$ [m/s]	Poisson ratio[ $\nu$ ]	L [G pa]	G [G pa]	B [G pa]	Y [G pa]
Original Sample	4.827	2.696	0.2773	383.98	119.78	224.27	305.04
Recycled Sample	5.446	2.707	0.3356	494.62	122.20	331.67	326.51

elastic moduli values L, B, G, and Y. This result attributed to the small size of the particles in the recycled sample enhanced the mechanical properties of the material in terms of its compactness, rigidity, and elastic behavior [21].

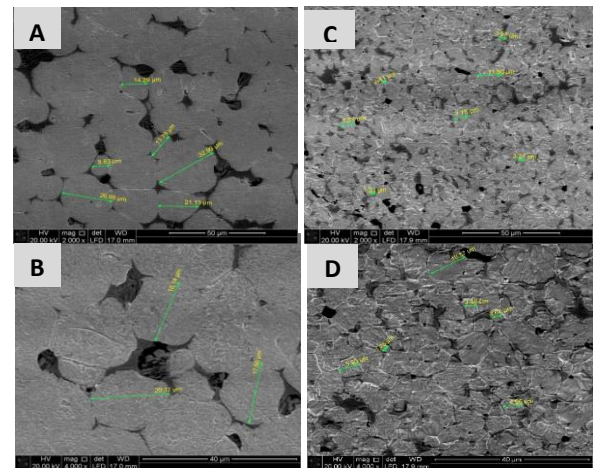


Figure 9. The microstructure under scanning electron microscope: A, B) The original sample at 2000X & 4000Xmag., C, D) The recycled sample at 2000X & 4000Xmag.

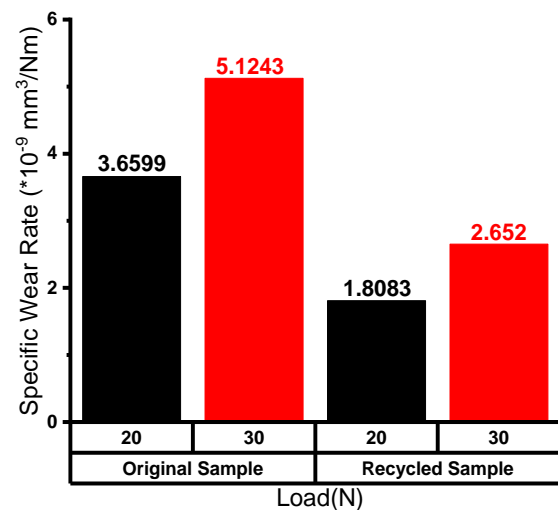


Figure 10. The Specific Wear Rate of original and recycled sintered tungsten heavy alloy (WHA)

**Table 2.** Coefficient of friction of original and recycled samples

Samples	Coefficient of friction at 20 N load	Coefficient of friction at 30 N load
Original sample	0.425	0.552
Recycled sample	0.403	0.426

## 5. Conclusion

This study has produced a novel technique for recycling tungsten metal powder from WHA wastes. Under the impact of ultrasonic waves, a significant amount of submicron tungsten powder was recovered from an acidic leach solution of tungsten alloy scrap. The outcome demonstrates that there was nine times as much tungsten powder recovered from the solution exposed to ultrasonic waves as there was powder recovered from the solution without ultrasonic waves. By using a powder metallurgy process, the recovered tungsten oxide powder is reduced and the nano tungsten metal powder is used to create the WHA alloy HA175. The physical and mechanical properties of the alloy formed from recycled tungsten powder are better than the original alloy as it shows an increase in density and hardness while the specific wear rate and coefficient of friction decreased.

## Data availability

All data generated or analyzed during this study are included in this published article

## Acknowledgment

My sincere thanks and appreciation to the Metals Research and Development Center (CMRDI) for helping me carry out this work in its laboratory.

## Reference

1. W. Liu, Q. Cai, Y. Ma, Q. Huang, and J. Zhang, *Fabrication of 93W-Ni-Fe alloy large-diameter rods by powder extrusion molding*. *Int J Refract Metals Hard Mater* (42) (2014)233–239. [https://doi: 10.1016/j.ijrmhm.2013.09.011](https://doi.org/10.1016/j.ijrmhm.2013.09.011).
2. R. Osama et al., *Effect of heat treatment on the mechanical properties and fracture behavior of tungsten heavy alloys*. *IJRET: International Journal of Research in Engineering and Technology* (6) (2017)140-144. <https://www.researchgate.net/publication/321775800>
3. R. K. Jana, V. Kumar, A. K. Saha, K. V Rao, and B. D. Pandey, *Processing of tungsten alloy scrap for the recovery of tungsten metal*. In: *Processing of National Seminar on Environmental & Waste Management in Metallurgical Industries, Jamshedpur* (1996)
4. O. G. Kuznetsova, A. M. Levin, M. A. Sevostyanov, O. I. Tsybin, and A. O. Bolshikh, *Electrochemical processing of heavy tungsten alloy wastes for obtaining a microdispersed iron-nickel base powder by using alternating current*. in *Journal of Physics: Conference Series*, IOP Publishing Ltd. (2021). [https://doi: 10.1088/1742-6596/1942/1/012056](https://doi.org/10.1088/1742-6596/1942/1/012056).
5. L. Luo et al., *Recovery of tungsten and vanadium from tungsten alloy scrap*. *Hydrometallurgy* (72) (2004) 1-2. [https://doi: 10.1016/S0304-386X\(03\)00121-X](https://doi.org/10.1016/S0304-386X(03)00121-X).
6. Z. Han, A. Golev, and M. Edraki, *A review of tungsten resources and potential extraction from mine waste*. *Minerals* (11) (7) (2021). [https://doi: 10.3390/min11070701](https://doi.org/10.3390/min11070701).
7. S. S. K. Kamal, J. Vimala, Y. Sushma, P. K. Sahoo, M. Sankaranarayana, and L. Durai, *Large scale synthesis of nanocrystalline tungsten powders through recycling of tungsten heavy alloy scrap*. *Mater Today Commun* (11) (2017) 174–178. [https://doi: 10.1016/j.mtcomm.2017.04.005](https://doi.org/10.1016/j.mtcomm.2017.04.005).
8. J. M. Pestman, J. B. F. N. Engberts, and F. De Jong, *Review Sonochemistry: theory and applications*. *Recueil des Travaux Chimiques des Pays-Bas* (113) (2010) 533-542. [https://doi:10.1002/recl.19941131202](https://doi.org/10.1002/recl.19941131202).
9. K. S. Suslick, *Sonochemistry science*. *Science* (247) (1990) 1439–1445.
10. N. E. Fouad, K. M. E. Attyia, and M. I. Zaki, *Thermogravimetry of WO<sub>3</sub>, reduction in hydrogen: kinetic characterization of autocatalytic effects*. *Powder Technology* (74) (1993) 31-37. [https://doi.org/10.1016/0032-5910\(93\)80005-U](https://doi.org/10.1016/0032-5910(93)80005-U).
11. G. L. Kehl, *The Principles of Metallographic Laboratory Practice*. *Engineering, Materials Science* (1949). <https://api.semanticscholar.org/corpusID:108600851>.
12. E. F. EL-kashif, S. A. Esmail, O. A. M. Elkady, B. S. Azzam, and A. A. Khattab, *Influence of carbon nanotubes on the properties of friction composite materials*. *J Compos Mater* (54) (16) (2020)2101–2111. [https://doi: 10.1177/0021998319891772](https://doi.org/10.1177/0021998319891772).
13. R. A. Elsad, A. M. Abdel-Aziz, E. M. Ahmed, Y. S. Rammah, F. I. El-Agawany, and M. S. Shams, *FT-IR, ultrasonic and dielectric characteristics of neodymium (III)/ erbium (III) lead-borate glasses: experimental studies*. *Journal of Materials Research and Technology* (13) (2021) 1363–1373. [https://doi: 10.1016/j.jmrt.2021.05.029](https://doi.org/10.1016/j.jmrt.2021.05.029).
14. H. A. Affi, I. Z. Hager, N. S. A. Aal, and A. M. Abd El-Aziz, *Study of the effect of Ni additive in YBa<sub>2</sub>Cu<sub>3</sub>O<sub>7-δ</sub> superconducting composite employing ultrasonic measurement*. *Measurement (Lond)* (135)(2019) 928–934. [https://doi: 10.1016/j.measurement.2018.12.006](https://doi.org/10.1016/j.measurement.2018.12.006).
15. O. G. Kuznetsova, A. M. Levin, M. A. Sevast'yanov, O. I. Tsybin, and A. O. Bol'shikh, *Electrochemical Oxidation of a Heavy Tungsten-Containing VNzh-Type Alloy and Its Components in Ammonia–Alkali Electrolytes*. *Russian Metallurgy (Metally)* (5)(2019) 507–510. [https://doi: 10.1134/S0036029519050057](https://doi.org/10.1134/S0036029519050057).
16. S. Sompech, A. Srion, and A. Nuntiya, *The effect of ultrasonic treatment on the particle size and specific surface area of LaCoO<sub>3</sub>*. in *Procedia Engineering, Elsevier Ltd* (2012) 1012–1018. [https://doi: 10.1016/j.proeng.2012.02.047](https://doi.org/10.1016/j.proeng.2012.02.047).



17. Z. A. Hamid, S. F. Moustafa, W. M. Daoush, F. A. Mouez, and M. Hassan, *Fabrication and Characterization of Tungsten Heavy Alloys Using Chemical Reduction and Mechanical Alloying Methods*. Open Journal of Applied Sciences (03) (2013) 15–27. [https://doi: 10.4236/ojapps.2013.31003](https://doi.org/10.4236/ojapps.2013.31003).
18. A. Imamović, Š. Žuna, E. Mulaosmanović, Z. Alibašić, and B. Kosec, *Comparison of mechanical and microstructure properties of tungsten alloys for special purposes*. Sustainable Engineering and Innovation (4) (2022)191–197. [https://doi: 10.37868/sei.v4i2.id180](https://doi.org/10.37868/sei.v4i2.id180).
19. Q. Wu, W. S. Miao, Y. Du Zhang, H. J. Gao, and D. Hui, *Mechanical properties of nanomaterials: A review*. Nanotechnol Rev (9) (2020) 259–273. [https://doi: 10.1515/ntrev-2020-0021](https://doi.org/10.1515/ntrev-2020-0021).
20. Z. Abidin, T. Nugroho, R. Tri Indrawati, E. Safriana, and F. Tono Putri, *Wear Rate Analysis Due to Dry Sliding Contact of Modified Rail to Increase Life Time in Air Blow Machine*. Jurnal Rekayasa Mesin (17)(2022) 151. [https://doi:10.32497/jrm.v17i1.3538](https://doi.org/10.32497/jrm.v17i1.3538).
21. S. A. Abdulsada and A. I. Al-Mosawi, *Mechanical Properties of Epoxy Nanocomposite*. International Journal of Advanced Research (6) (2015)1468-1472. ISSN 2320-5407